Chinese Chemical Letters 31 (2020) 774–778

Contents lists available at ScienceDirect

Chinese Chemical Letters

journal homepage: www.elsevier.com/locate/cclet

Communication

MOF derived Co_3O_4/N-doped carbon nanotubes hybrids as efficient catalysts for sensitive detection of H_2O_2 and glucose

Yingnan Qin[a,b], Yingjun Sun[a,b], Yingjie Li[b], Chunji Li[b], Lei Wang[a,*], Shaojun Guo[b,*]

[a] College of Chemistry and Molecular Engineering, Qingdao University of Science and Technology, Qingdao 266042, China
[b] Department of Materials Science and Engineering, Department of Biomedical Engineering, College of Engineering, Peking University, Beijing 100871, China

ARTICLE INFO

Article history:
Received 12 June 2019
Received in revised form 4 September 2019
Accepted 9 September 2019
Available online 11 September 2019

Keywords:
ZIF-67
Co_3O_4/NCNTs hybrids
Enzyme-free sensor
H_2O_2
Glucose

ABSTRACT

Developing enzyme-free sensors with high sensitivity and selectivity for H_2O_2 and glucose is highly desirable for biological science. Especially, it is attractive to exploit noble-metal-free nanomaterials with large surface area and good conductivity as highly active and selective catalysts for molecular detection in enzyme-free sensors. Herein, we successfully fabricate hollow frameworks of Co_3O_4/N-doped carbon nanotubes (Co_3O_4/NCNTs) hybrids by the pyrolysis of metal-organic frameworks followed by calcination in the air. The as-prepared novel hollow Co_3O_4/NCNTs hybrids exhibit excellent electrochemical performance for H_2O_2 reduction in neutral solutions and glucose oxidation in alkaline solutions. As sensor electrode, the Co_3O_4/NCNTs show excellent non-enzymatic sensing ability towards H_2O_2 response with a sensitivity of 87.40 μA $(mmol/L)^{-1}$ cm^{-2}, a linear range of 5.00 μmol/L–11.00 mmol/L, and a detection limitation of 1 μmol/L in H_2O_2 detection, and a good glucose detection performance with 5 μmol/L. These excellent electrochemical performances endow the hollow Co_3O_4/NCNTs as promising alternative to enzymes in the biological applications.

The efficient detection of hydrogen peroxide and glucose has triggered increasing attentions due to their important roles in food industry, fuel cells and especially in clinical diagnostics [1–3]. The concentrations of H_2O_2 and glucose in biological bodies are closely related to physiological health, such as diabetes, Parkinson and myocardial infarction [4–6]. The real-time detection of H_2O_2 and glucose in biological bodies is beneficial to not only discovering the inherent small molecule-disease relationship, but also diagnosing diseases timely and accurately along with monitoring the disease progression [7]. Nowadays, the electrochemical method becomes increasingly popular for sensor research because of the simple operation, high sensitivity, and fast response [8,9], compared with other detective technologies including colorimetric [10], spectrophotometric [11] and surface plasmon resonance methods [12]. Normally, the reliability of electrochemical sensors, which is classified into enzyme-based and enzyme-free sensors, strongly depended on the electrode materials which are expected to be highly active to target small molecules. Although the enzyme-based sensors show excellent selectivity and outstanding sensitivity for target small molecular, their disadvantages include high cost, complicated operation, and the intrinsic properties affected easily by environment factors hinder the scale-up application [13,14]. Considering the above-mentioned, it is highly desirable to develop enzyme-free sensors with high selectivity and sensitivity based on the consideration of economy.

In literatures, noble metal (NM) based materials have been widely demonstrated to be a class of excellent enzyme-free electrochemical sensors due to their high sensitivity [15,16]. However, the low natural abundance and high cost greatly impede their widely adoption. Recently, cost-efficiency transition metal oxides, such as Co_3O_4–rGO [17], CuO-SiNWs [18], Fe_3O_4 [19], have being studied as enzyme-free and NM-free electrochemical sensors for small molecules. But the poor conductivity and easy aggregation of the transition metal oxides could reduce the activity sites, and limit the kinetics of the catalytic process. Thus, the emergence of transition metal oxides/carbon hybrids [20–22] could efficiently prevent the aggregation and improve the conductivity of the catalysts. Therefore, the structural design of transition metal oxides-based sensor should be given considerations to the following aspects: (1) Sensitivity. Take advantages of the good redox performance of transition metal oxides, explore more active sites of the catalysts. (2) Electron and mass transfer. Arranging the conductive carbon materials in an ordered manner could facilitate the transfer of both electrons and target molecules.

Herein, we fabricate hollow frameworks of Co_3O_4/nitride-doped carbon nanotubes (Co_3O_4/NCNTs) hybrids derived from

* Corresponding authors.
E-mail addresses: inorchemwl@126.com (L. Wang), guosj@pku.edu.cn (S. Guo).

https://doi.org/10.1016/j.cclet.2019.09.016
1001-8417/

MOFs as an efficient catalyst for the electrochemical detection of H_2O_2 and glucose. Firstly, the Co_3O_4 nanoparticles can provide active sites for enzyme-free detection, improving the activity of the catalysts. Secondly, the *in-situ* formed carbon nanotube frameworks can improve the electronic conductivity, and facilitate the mass transfer of target molecules. Thirdly, the coated carbon shells can effectively immobilize the oxide nanoparticles and, thus suppress the aggregation. This study opens a new avenue for developing cost-efficiency yet high-performance electrochemical sensors *via* rationally structural design.

The synthesis of the catalysts was followed by the reported method [23]. The dodecahedral ZIF-67 nanoparticles (Fig. S1 in Supporting information) were selected as the precursor and self-sacrificing template to prepare the Co/NCNTs and Co_3O_4/NCNTs. The Co/NCNTs were obtained by simply carbonizing the ZIF-67 under the H_2/Ar atmosphere. As shown in Fig. S2 (Supporting information), the polyhedral structure can be well retained after thermal annealing, despite of the notably roughness and concaveness on the surface of Co/NCNTs. Close inspection by TEM (Figs. S2b and S2d) on Co/NCNTs reveals that high density of carbon nanotubes array on the surface of hollow dodecahedrons, with the terminal of each nanotube encapsulating a Co particle. Then, the Co/NCNTs were converted into Co_3O_4/NCNTs by keeping at 150 °C under air for 12 h in an oven. Both TEM and SEM images (Figs. 1a–d) show a greatly swelling in size after the above oxidation treatment. The crystalline nature of the product can be further confirmed by XRD. Fig. 1e shows the XRD patterns of Co/NCNTs (the blue line) and Co_3O_4/NCNTs (the red line). The main peaks marked with triangles in Co/NCNTs are assigned to Co (Co# JCPDS No. 15-0806). After oxidation treatment, the characteristic peaks of Co are disappeared, the main peaks marked with stars are in accord with the Co_3O_4 (Co_3O_4# JCPDS No. 43-1003). X-ray photoelectron spectroscope (XPS) was carried out to identify the surface valence states of the products (Fig. 1f). The major peaks at 794.6 and 779.2 eV were in accordance with Co $2p_{1/2}$ and Co $2p_{3/2}$, respectively. The two weak peaks at 803.3 eV and 786.7 eV (marked by S) can be further confirmed as the satellite peaks of Co oxidation state. The red peak in Co/NCNTs indicates the Co metallic state, and this peak was disappeared after oxidation treatment, suggesting that the Co(0) has turned into Co oxides completely. The elements distribution of Co_3O_4/NCNTs (Fig. 1g) and Co/NCNTs (Fig. S3a in Supporting information) conducted by EDS mapping shows that the Co, C and N distributed uniformly in the samples. To understand the bonding environment of the elements, high resolution XPS spectrums of C 1s and N 1s have been taken. As shown in Fig. S3b (Supporting information), the peak at 284.5 eV is related to the sp^2 carbon and the peak at 285.7 eV is related to combination of sp^3 carbon and C–N bonding. As shown in Fig. S3c (Supporting information), the peaks at 398.2, 399.8, and 400.9 eV are related to pyridinic, pyrrolic, and graphitic nitrogen, which could suggest the existence of nitride-doped carbon structure. Raman spectrum of the Co/NCNTs was shown in Fig. S3d (Supporting information). The peaks at 1337.5 and 1580.6 cm^{-1} were assigned to the characteristic G (graphite band) and D (defect band) bands of carbon. The D band demonstrated the doping of N and Co in the carbon nanotubes, and the G band includes the vibrations of carbon atoms along and around the circumference of the nanotube. The I_D/I_G is 1.20, which indicates the strong doping effect in the Co/NCNTs [24].

The enzyme-free H_2O_2 electrochemical detection is conducted in a traditional three-electrode system by the CHI 660e electrochemical workstation (Shanghai Chenhua Instrument Corporation, China). In our study, we use 0.1 mol/L PBS solution (pH 7.4) as the electrolyte. Fig. 2a depicts the cyclic voltammograms of Co/NCNTs and Co_3O_4/NCNTs modified electrodes in 0.1 mol/L PBS containing

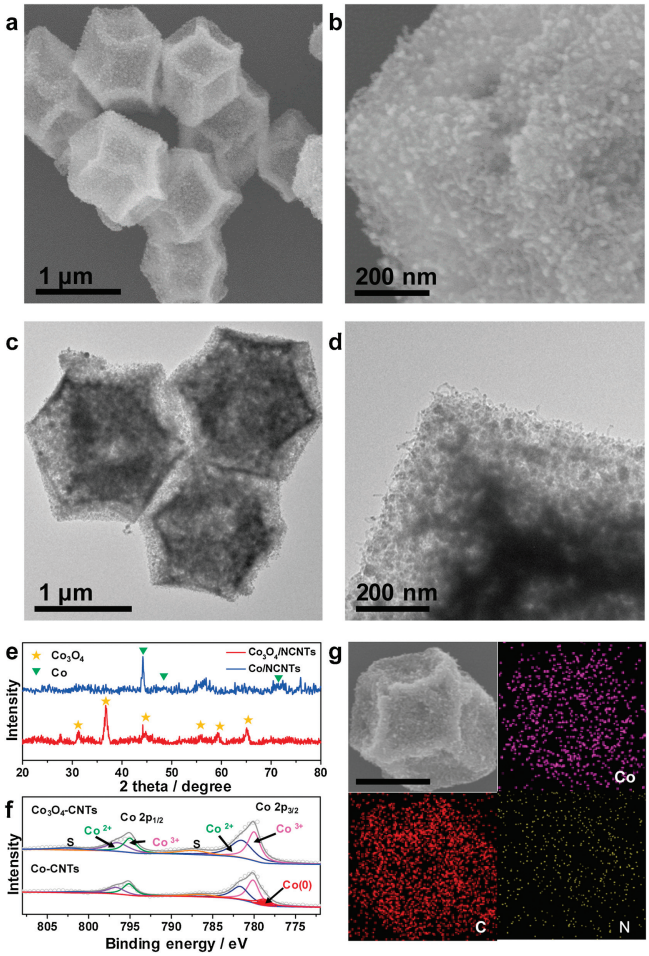

Fig. 1. (a and b) Typical SEM images of Co_3O_4/NCNTs; (c and d) Typical TEM images of Co_3O_4/NCNTs; (e) XRD pattern of Co_3O_4/NCNTs and Co/NCNTs; (f) XPS patterns of Co_3O_4/NCNTs and Co/NCNTs; (g) SEM element mapping of Co_3O_4/NCNTs (the scale bar is 500 nm).

1 mmol/L H_2O_2. A series of CVs were recorded on Co_3O_4/NCNTs modified GCE at various H_2O_2 concentrations (0, 0.1, 0.2, 0.5, 1.0, 1.5, 2.0 and 3.0 mmol/L) (inset in Fig. 2b). The cathodic current increases obviously with the addition of H_2O_2, and the peak current is in good linear relationship with the H_2O_2 concentration (Fig. 2b). According to the previous reports, the electrocatalysis of H_2O_2 on the Co_3O_4/NCNTs can be expressed by the following Eq. (1) [18]:

$$2Co(III) + H_2O_2 + 2OH^- \rightarrow 2Co(II) + O_2 + 2H_2O \quad (1)$$

The electrochemical process of H_2O_2 on the Co_3O_4/NCNTs modified GCE was studied in 0.1 mol/L PBS buffer solution (pH 7.4) containing 0.1 mol/L H_2O_2 at different scan rate (50, 80, 100, 150, 200, 250, 300, 400 and 500 mV/s) (Fig. 2c). We can further find that the current at 0.0 V *versus* Ag/AgCl can be in good linear with the square root of the scan rates (Fig. 2d), which indicate that the H_2O_2 oxidation on the Co_3O_4/NCNTs modified electrode was a typical diffusion-controlled process.

The optimal potential can be found by amperometric technology at different applied potentials with the successive addition of 0.2 mmol H_2O_2 (Fig. S4a in Supporting information). Fig. S4b (Supporting information) shows the calibration curve of current at different applied potentials (−0.15 V, −0.20 V and −0.25 V *versus* Ag/AgCl). We can find that the most sensitive current respond is occurred at −0.20 V *versus* Ag/AgCl, so we select −0.20 V as the best applied potential for further use. Compared with Co/NCNTs

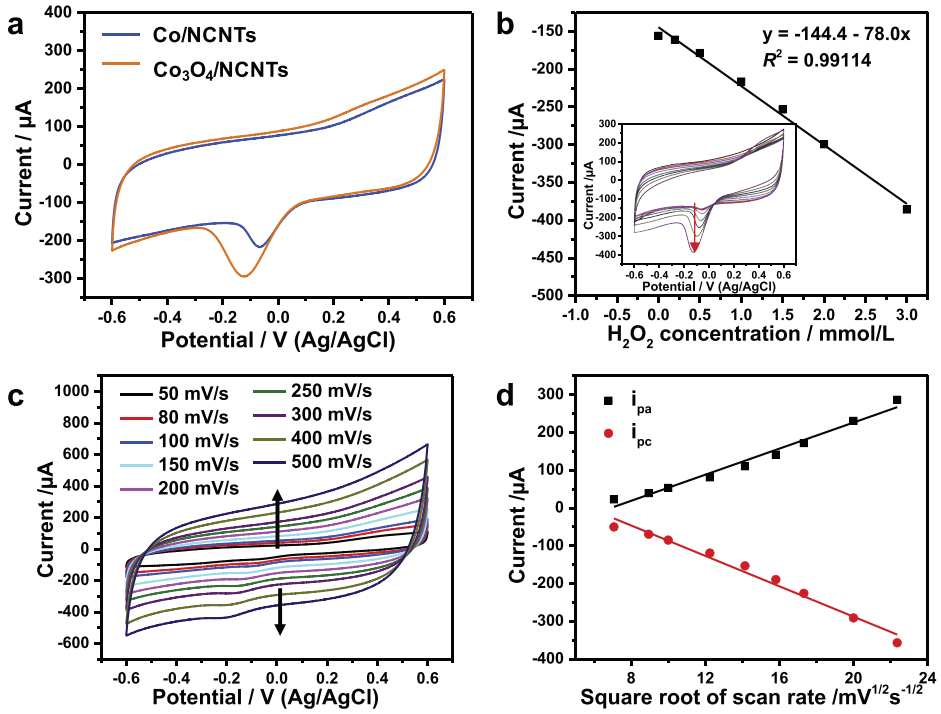

Fig. 2. (a) CVs of Co/NCNTs and Co_3O_4/NCNTs electrodes in 0.1 mol/L PBS (pH 7.4) with 1 mmol/L H_2O_2; (b) Calibration curve of the amperometric response to the concentration of H_2O_2 from 0 to 3.0 mmol/L; (c) CVs of the Co_3O_4/NCNTs electrode in N_2-saturated 0.1 mol/L PBS (pH 7.4) with 0.1 mmol/L H_2O_2 at different scan rate (50, 80, 100, 150, 200, 250, 300, 400, and 500 mV/s). (d) Calibration curve of the amperometric response to the square root of scan rate. The inset in (b) shows CVs of the Co_3O_4/NCNTs electrode in N_2-saturated 0.1 mol/L PBS (pH 7.4) in the absence and presence of H_2O_2 with different concentrations (Scan rate: 100 mV/s).

modified GCE, the Co_3O_4/NCNTs modified GCE has a higher sensitivity. The sensitivity of Co_3O_4/NCNTs is evaluated to be 87.40 μA $(mmol/L)^{-1}$ cm^{-2} through the linear calibration curve.

Fig. 3a shows the amperometric response to successive injection of various concentration of H_2O_2 into the 0.1 mol/L PBS buffer solution (pH 7.4) at an applied potential of −0.2 V *versus* Ag/AgCl. It is found that the current of Co_3O_4/NCNTs modified GCE increases rapidly with the successive addition of H_2O_2, and only take few seconds to obtain a new current platform. The calibrated curve of current and concentration (Fig. 3b) shows that there is a

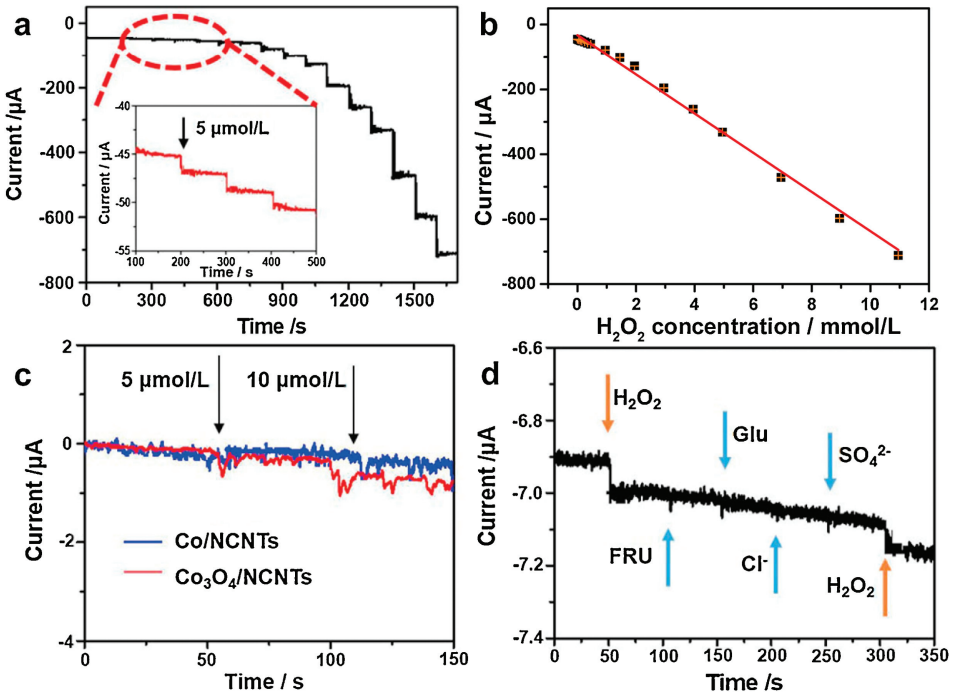

Fig. 3. (a) Amperometric responses of the Co_3O_4/NCNTs electrode to the successive addition of H_2O_2 in PBS at an applied potential of −0.2 V *versus* Ag/AgCl; (b) Dependence of the response of the electrode on H_2O_2 concentration; (c) Amperometric responses of Co/NCNTs and Co_3O_4/NCNTs with the addition of the same concentration H_2O_2; (d) Amperometric response of the Co_3O_4/NCNTs electrode at −0.2 V for the sequential addition of 0.2 mmol/L H_2O_2, FRU, Glu, Cl^- and SO_4^{2-} into 0.1 mol/L PBS (pH 7.0). The inset of (a) shows the close look of the red circle with the H_2O_2 concentration of 5 μmol/L.

linear range from 5.00 μmol/L to 11.00 mmol/L. The detection limitation of Co_3O_4/NCNTs is conducted by signal-to-noise ratio (S/N = 3) is 1 μmol/L through amperometric test. Fig. 3c depicts the amperometric response of Co/NCNTs and Co_3O_4/NCNTs with the same addition of H_2O_2. The Co_3O_4/NCNTs is more sensitive than Co/NCNTs. The results indicate that the Co_3O_4/NCNTs can enable accelerate the adsorption and activation of H_2O_2 molecules. As recorded in Table S1 (Supporting information), compared with other reported H_2O_2 sensors, our Co_3O_4/NCNTs shows a larger linear range and a lower detection limitation. Although, some electrodes exhibit a higher sensitivity, the narrow detection range could limit the practical application. Thus, the Co_3O_4/NCNTs could be used as an excellent catalyst for enzyme-free H_2O_2 sensors. The selectivity is another important parameter to evaluate the performance of the catalysts, especially in the practical application. In this work, we investigated the co-existence of other interfering species with H_2O_2 (GLU, FRU, Cl^- and SO_4^{2-}). As shown in Fig. 3d, the *i–t* curve was conducted by successive injection of 2 mmol/L H_2O_2 and interfering species at an applied potential of −0.2 V (*versus* Ag/AgCl). There is a negligible current response to the addition of the interfering species. The excellent selectivity of Co_3O_4/NCNTs for H_2O_2 detection can be ascribed to the negative potential that the interfering species cannot conduct electrochemical reaction.

The Co_3O_4/NCNTs are also active for enzyme-free glucose detection. Fig. 4a depicts the cyclic voltammograms of Co/NCNTs and Co_3O_4/NCNTs modified electrodes in 0.1 mol/L NaOH containing 1 mmol/L glucose. The inset of Fig. 4b shows the CVs of the Co_3O_4/NCNTs modified GCE in 0.1 mol/L NaOH solutions containing various glucose concentrations. The anodic currents at 0.6 V (*versus* Ag/AgCl) are in good linear relationship with the glucose concentrations (Fig. 4b). CV curves at different scan rate in 0.1 mol/L NaOH containing 1 mmol/L glucose have been measured (Fig. S5a in Supporting information). The current at 0.6 V *versus* Ag/AgCl can be in a good linear with the square root of scan rates (Fig. S5b in Supporting information), which indicates that the glucose oxidation on the Co_3O_4/NCNTs modified electrode was a typical diffusion-controlled process.

Amperometric technology has been taken to find the optimal potential by successive addition of 0.2 mmol/L glucose at different applied potential (Fig. S5c in Supporting information). The calibration curves show that 0.6 V *versus* Ag/AgCl is the best potential for further use. The sensitivity of Co_3O_4/NCNTs is evaluated to be 86.6 μA $(mmol/L)^{-1}$ cm^{-2} through the linear calibration curve (Fig. S5d in Supporting information). Fig. 4c shows the amperometric response to successive injection of various concentration of glucose into the 0.1 mol/L NaOH solution at an applied potential of 0.6 V *versus* Ag/AgCl. The rapid current response indicates the good detection performance. The calibrated curve (inset in Fig. S6d in Supporting information) shows that there are two linear ranges, which are 5.00 μmol/L–2.65 mmol/L and 4.65–13.65 mmol/L. The two linear ranges are caused by different glucose absorption and activation behavior on the Co_3O_4/NCNTs modified GCE under different glucose concentrations. The selectivity of glucose was conducted by chronoamperometry at 0.6 V (*versus* Ag/AgCl). The *i–t* curve of successive addition of 2 mmol/L glucose and other interfering substances (Cl^-, SO_4^{2-}, K^+, Mg^{2+} and EtOH) was shown in the inset of Fig. 4d. The current gets an obvious increase with the injunction of glucose, and no responses of the injunction of the interfering substances, indicating that the excellent selectivity of Co_3O_4/NCNTs for glucose detection. The detection limitation of Co_3O_4/NCNTs is 5 μmol/L through amperometric test. With the same addition of glucose, Co_3O_4/NCNTs is sensitive than Co/NCNTs (Fig. 4d), indicating that

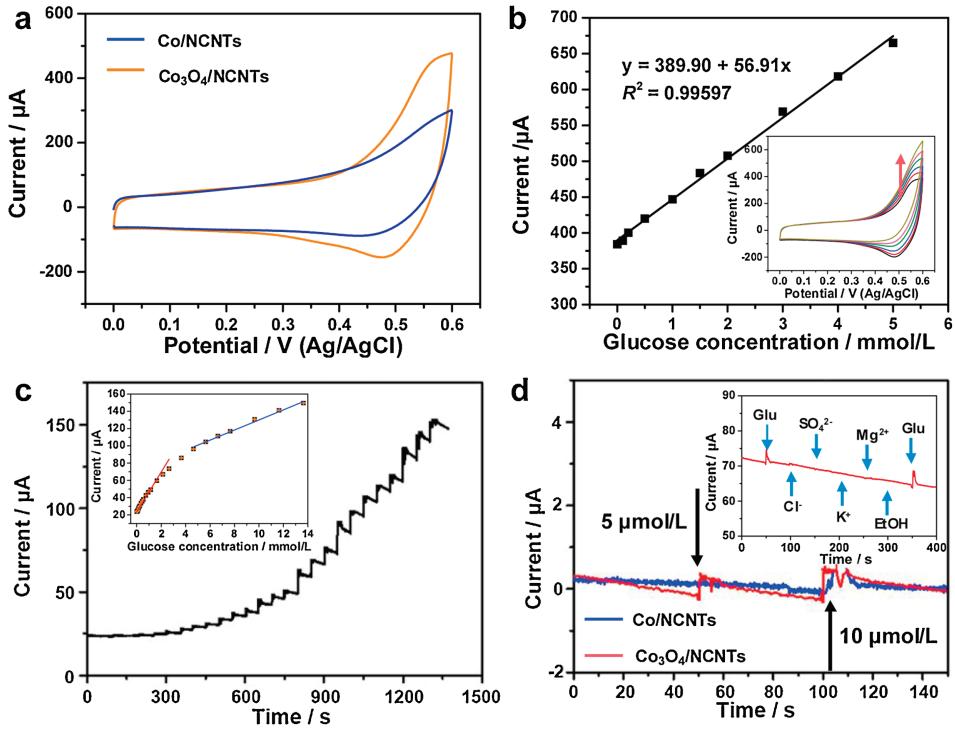

Fig. 4. (a) CVs of Co/NCNTs and Co_3O_4/NCNTs electrodes in 0.1 mol/L NaOH without or with 1 mmol/L glucose; (b) Calibration curve of the amperometric response to the concentration of glucose from 0 to 3.0 mmol/L; (c) Amperometric responses of the Co_3O_4/NCNTs electrode to the successive addition of glucose in NaOH at an applied potential of 0.6 V *versus* Ag/AgCl; (d) Amperometric responses of Co/NCNTs and Co_3O_4/NCNTs with the addition of the same concentration glucose. The inset in (b) shows CVs of the Co_3O_4/NCNTs electrode in 0.1 mol/L NaOH in the absence and presence of glucose with different concentrations (Scan rate: 100 mV/s). The inset in (c) shows the dependence of the response of the electrode on glucose concentration. The inset in (d) shows the amperometric response of the Co_3O_4/NCNTs electrode at 0.6 V for the sequential addition of 0.2 mmol/L Glu, Cl^-, SO_4^{2-}, K^+, Mg^{2+} and EtOH into 0.1 mol/L NaOH.

the Co_3O_4 has a higher detective ability towards glucose, probably because the glucose can be oxidized more easily by the high valence cobalt. Compared with other glucose and glucose oxidase immobilized sensors (Table S2 in Supporting information), the glucose detection performance of our Co_3O_4/NCNTs is better than those of other sensors. The Co_3O_4/NCNTs have a lower detection limitation, better sensitivity and larger linear range than glucose oxidase immobilized sensors. Thus, the Co_3O_4/NCNTs are excellent for enzyme-free glucose detection.

In summary, the Co_3O_4/NCNTs were prepared by simply pyrolyzing the ZIF-67 precursor in H_2/Ar atmosphere. The ZIF-67 derived Co_3O_4/NCNTs is an excellent catalytic material for the enzyme-free sensor, which is related to the special structure. Firstly, the Co_3O_4 can provide more active sites and improve the activity. Secondly, the conductive carbon nanotubes can cover the poor conductivity of Co_3O_4 nanoparticles, which can facilitate the transfer of both electrons and target molecules and prevent the aggregation of Co_3O_4 nanoparticles. The Co_3O_4/NCNTs modified electrode exhibit excellent electrochemical performance towards H_2O_2 detection, with a sensitivity of 87.40 μA $(mmol/L)^{-1}$ cm^{-2}, a linear range of 5.00 μmol/L-11.00 mmol/L, and a detection limitation of 1 μmol/L. Although, there are still lots of challenges in the practicability of enzyme-free electrochemical sensor, the Co_3O_4/NCNTs is a promising candidate in this field.

Acknowledgments

This work was financially supported by the National Natural Science Foundation of China (NSFC) (Nos. 51671003, 21802003, 21571112), Natural Science Foundation of Shandong Province (ZR2018BB031), the Shandong Taishan Scholar Program (H.W.), the China Postdoctoral Science Foundation (No. 2017M610022), the start-up supports from Peking University and Young Thousand Talented Program.

Appendix A. Supplementary data

Supplementary material related to this article can be found, in the online version, at doi:https://doi.org/10.1016/j.cclet.2019.09.016.

References

[1] J.S. Chung, S.H. Hur, Sens. Actuators B-Chem. 223 (2016) 76–82.
[2] Meng, Y. Wen, L. Dai, et al., Sens. Actuators B-Chem. 260 (2018) 852–860.
[3] H. Heidari, E. Habibi, Microchim. Acta 183 (2016) 2259–2266.
[4] Y. Sun, M. Luo, Y. Qin, et al., ACS Appl. Mater. Interfaces 9 (2017) 34715–34721.
[5] J. Mu, L. Zhang, M. Zhao, et al., ACS Appl. Mater. Interfaces 6 (2014) 7090–7098.
[6] B. Dou, J. Yang, R. Yuan, et al., Anal. Chem. 90 (2018) 5945–5950.
[7] H. Cheng, L. Zhang, J. He, et al., Anal. Chem. 88 (2016) 5489–5497.
[8] L. Tian, G. He, Y. Cai, et al., Nanotechnology 29 (2018) 075502.
[9] Y. Su, B. Luo, J.Z. Zhang, Anal. Chem. 88 (2016) 1617–1624.
[10] C. Gao, H. Zhu, J. Chen, et al., Chin. Chem. Lett. 28 (2017) 1006–1012.
[11] M. Song, J. Wang, B. Chen, et al., Anal. Chem. 89 (2017) 11537–11544.
[12] A. Amirjani, M. Bagheri, M. Heydari, et al., Sens. Actuators B-Chem. 227 (2016) 373–382.
[13] C. Chen, X. Hong, T. Xu, et al., Synthetic Met. 212 (2016) 123–130.
[14] H. Quan, C. Zuo, T. Li, et al., Electrochim. Acta 176 (2015) 893–897.
[15] C. Chen, R. Ran, Z. Yang, et al., Sens. Actuators B-Chem. 256 (2018) 63–70.
[16] C.L. Yang, X.H. Zhang, G. Lan, et al., Chin. Chem. Lett. 25 (2014) 496–500.
[17] Kong, Z. Ren, N. Zheng, et al., Nano Res. 8 (2015) 469–480.
[18] J. Huang, Y. Zhu, H. Zhong, et al., ACS Appl. Mater. Interfaces 6 (2014) 7055–7062.
[19] J. Yang, H. Xiang, L. Shuai, et al., Anal. Chim. Acta 708 (2011) 44–51.
[20] C. Zhang, L. Li, J. Ju, et al., Electrochim. Acta 210 (2016) 181–189.
[21] H. Dai, Y. Chen, X. Niu, et al., Biosens. Bioelectron. 118 (2018) 36–43.
[22] X. Feng, Y. Zhang, J. Song, et al., Electroanalysis 27 (2015) 353–359.
[23] B.Y. Xia, Y. Yan, N. Li, et al., Nat. Energy 1 (2016) 15006.
[24] G.J.H. Melvin, Q.Q. Ni, Y. Suzuki, et al., J. Mater. Sci. 49 (2014) 5199–5207.